RSC Advances

ROYAL SOCIETY OF CHEMISTRY

www.rsc.org/advances

Journal Name

RSCPublishing

ARTICLE

Eu doped Si-Oxynitride fluorescent nanofibrous inorganic membranes with high flexibility

Cite this: DOI: 10.1039/

Hailei Zhao,[a] Bo Cui,[a] Zhenhua Chen,[a] Hongzhi Wang,*[a] Qinghong Zhang[a] and Yaogang Li*[b]

Pure inorganic materials are expected to find applications in various fields including energy-efficient and environmental-friendly soft display technologies, thereby requiring them to operate effectively while being bent or stretched. In the present study, excellent mechanical flexibility properties were successfully imparted into conventionally fragile inorganic materials using a nanobelt network design. Specifically, organic-inorganic composite materials were engineered into considerably long and continuous nanobelts using a simple electrospinning process. The composites were then subjected to calcination and nitridation processes to produce highly fluorescent inorganic (Si-based) membranes with high flexibility. The synthesized nanobelts exhibits high aspect ratios and well-defined rectangular cross-sections, and displays excellent mechanical flexibility. The nanobelts could be bent to minimum curvature radius down to 1 mm. Furthermore, the nanobelts incurs no visible damage after 500 cycles of bending to a radius of 1 cm. Under an applied strain of 6% for 500 cycles, the flexible SiO2-based fluorescent nanobelt membrane maintained a high strength of 6.0 MPa. Moreover, the photoluminescence intensity of the free-standing fluorescent nanofibrous inorganic membranes featured excellent environmental, thermal and mechanical cyclic stability. The current findings strongly indicate the great potential of the engineered fluorescent inorganic membranes as fluorescent materials in flexible display technologies and the remote packaging of LED.

Received ooth
Accepted ooth

DOI: 10.1039/xoxxooooox
www.rsc.org/

1. Introduction

Due to their excellent chemical and thermal stabilities, inorganic materials have been employed as key components in various applications, such as in displays,[1,2] light-emitting diodes,[3-5] field-effect transistors,[6] filter materials,[7] and sensors.[8,9] However, their applications in flexible displays is severely limited because of their powder shape and brittleness.

With the development of technology, the electrospinning of nanofibrous inorganic membranes has attracted great interest.[10] Electrospinning offers a simple, versatile and cost-effective method for controlling the morphology and arrangement of fibers with diameters ranging from tens of nanometers up to micrometres. Owing to the progress made to date, various materials can be electrospun into uniform fiber membranes or mats.[11-13] Fibers prepared by electrospinning have several benefits such as good orientation, large specific surface area, and high aspect ratio. Furthermore, among the fibers development, luminescent electrospun nanofibers have attracted great attention recently. Examples of such types of fibers are made of $YBO_3:Eu^{3+}$,[14] $CaWO_4:Tb^{3+}$,[15] $Sr_2SiO_4:Eu^{3+}$,[16] and $LaOCl:Eu^{3+}$.[17]

Although the considerable progress has been achieved to date on the electrospinning of fluorescent inorganic materials. The fabrication of fluorescent inorganic materials with excellent deformability in a scalable fashion still remains a great challenge. Moreover, the efficient integration of such materials, with improved mechanical flexibility into flexible functional devices, especially on substrates with different textures and complex surfaces, is far from being well developed.[18] Therefore, the development of flexible fluorescent nanofibrous inorganic membranes is of great challenge for their practical applications.

Some groups have reported the preparation of fluorescent oxynitride glass by melting batches at 1550□ under N_2 atmosphere. Relative, to oxide glass, fluorescent oxynitride glass features higher glass transition temperature, microhardness, bending strength, elastic modulus, fracture toughness, and refractive index, and a lower thermal expansion coefficient. Furthermore, such a fabrication process enables the

[a]*State Key Laboratory for Modification of Chemical Fibers and Polymer Materials, College of Materials Science and Engineering, Donghua University, Shanghai 201620, Email:wanghz@dhu.edu.cn;*

[b]*Engineering Research Cebnter of Advanced Glasses Manufacturing Technology, Donghua University, Shanghai 201620, China. Email: yao gang_li@dhu.edu.cn;*

preparation of fine appearance, homogeneous, translucent, and defect-free bulk oxynitride glass. However, further increases in the heat-treatment temperature to over 1550□ led to a sharp decrease in the mechanical strength of the fluorescent oxyntride glass.[19-24] In this study, novel flexible SiO_2-based fluorescent nanobelt membranes (FNMs) were fabricated via electro-spinning combined with gas-reduction nitridation. The current findings strongly indicate the great potential of the engineered fluorescent inorganic membranes as fluorescent materials in flexible display technologies and the remote packaging of LED.

2. Experimental

2.1. Materials

$Ca(NO_3)_2{\cdot}4H_2O$ (99.9%) and $Eu(NO_3)_3{\cdot}6H_2O$ (99.9%) were obtained from Shanghai Diyang Chemical Ltd. Tetraethyl orthosilicate $Si(OC_2H_5)_4$ (TEOS, 99 wt.%, analytical reagent, A. R., Sinopharm Chemical Reagent Co., Ltd.), and poly vinyl butyral (PVB, 15-35mm^2/s, Sinopharm Chemical Reagent Co., Ltd.).

2.2. Fabrication of nanobelt structure of FNMs

Fig. 1 illustrates the equipment employed for preparing the membrane, whereby the precursor solution containing the inorganic source and polymer was spun using a syringe under a high voltage electric field. The obtained product was then calcined in air and nitrided in pure NH_3 flow. Specifically, 3.4 mmol $Ca(NO_3)_2{\cdot}4H_2O$, 0.17 mmol $Eu(NO_3)_3{\cdot}6H_2O$, and 20 mL TEOS were dissolved in 40 mL of a mixed solution comprising ethanol and deionized water solution (v/v = 7:1) under magnetic stirring for 1 h. Then, a certain amount of PVB was added to adjust the viscoelasticity of the above-prepared solution (the weight percentage of PVB in the deionized water/ethanol mixed solution was 6%). The resulting solution was stirred for 1 h to obtain a homogeneous hybrid solution for subsequent electrospinning. The as-prepared precursor solution was loaded into a 10 mL syringe. The anode of the high-voltage power supply was clamped to the syringe needle tip, and the cathode was connected to the grounded collector plate. The applied voltage was 16 kV, and the distance between the needle tip and the collector was 21 cm. The flow rate of the spinning solution was controlled at 0.5 mL h^{-1} by a syringe pump (Model 22, Harvard Apparatus, USA).

The as-prepared FNM was first heated from room temperature to 500 □ under air atmosphere at a heating rate of 1 □ min^{-1}, after which the temperature was maintained at 500 □for 2 h to decompose PVB. Subsequently, the resulting product was introduced into a high-temperature tube furnace, and heated to 700 □ under air atmosphere using a heating rate of 2 □ min^{-1}, after which the temperature was maintained for 2 h. Then the nitridation process was initiated by increasing the temperature to 1000□, 1100□,1200□ or 1300□ under pure NH_3 flow (300 mL min^{-1}). The temperature was maintained for 5 h. Finally, the sample was cooled to room temperature under NH_3 atmosphere to produce a flexible self-supporting FNM. For comparison, pure silica and PVB fiber membranes without the addition of $Ca(NO_3)_2{\cdot}4H_2O$ or $Eu(NO_3)_3{\cdot}6H_2O$ were prepared under the same conditions.

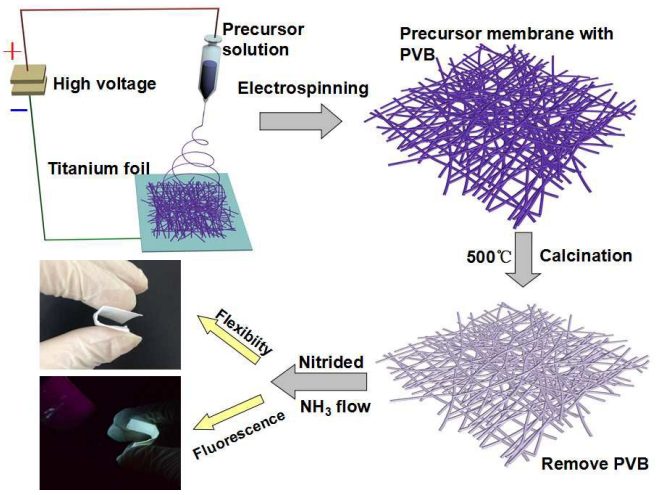

Fig. 1 Schematic illustration of the fabrication process of the free-standing fluorescent inorganic nanofibrous membranes.

.

2.3 Characterization

The surfaces of the PVB, PVB/SiO_2 and SiO_2 fiber membranes were analyzed by Fourier transform infrared (FT-IR) spectroscopy. Thermogravimetric analysis (TGA) of the SBFNM (precursor fiber membrane) was conducted on a Nezsch TG 209F1 analyzer. For the analysis, a few milligrams of the samples were heated at a heating rate of 10 □ min^{-1} from room temperature to 900 □ under air atmosphere. The surface morphology of the network was examined by field-emission scanning electron microscopy (FESEM) on a JSM5600LV microscope operating at 5.0 kV. The photoluminescence (PL) spectra were measured at room temperature on a fluorescence spectrophotometer (JASCO FP-6600). The phase formation and crystal structure were analyzed by X-ray diffraction (Rigaku-D/max 2550 PC diffractometer) with Cu-Kα radiation (λ = 0.10405 nm).

3. Results and discussion

3.1 Characterization of precursor membrane

The preparation of the FNMs is tunable and easy to scale-up by simply adjusting electrospinning parameters, such as area of collector (Fig. S1) and electrospinning time (Fig. S2). Fig. 2a shows a digital photo of the FNM precursor membrane. As observed, the nanobelt-like membrane was smooth, uniform and big as the palm with dimensions of 400 cm^2. By increasing the electrospinning time, nanobelt membranes with different thicknesses could be obtained. The SEM image in Fig. 2b shows a representative cross-sectional view of a FNM obtained

after 10 h of electrospinning: the thickness of the membrane is 180 μm. The low- and high-magnification images in Fig. 2c and d show that the FNM is composed of intertwined uniform fibers with an average diameter of 500 nm.

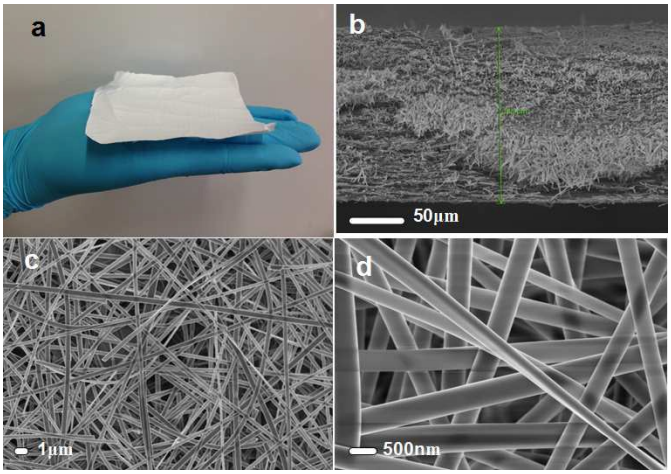

Fig. 2 (a) Optical image of the FNM precursor membrane. (b) Cross-sectional view of FNM obtained after 10 h of electrospinning: the thickness is 180 μm as indicated by the arrow. (c) Low-magnification scanning electron microscopy (SEM) image of FNM composed of intertwined uniform fibers. (d) High-magnification SEM image revealing that the average diameter of FNM is 500 nm.

The formation mechanism of a nanobelt fiber could be explained as follows: the rate of solvent evaporation on thesurface of the extruded electrospinning precursor solution is higher than that in the inner region of the extruded precursor solution, thereby forming a skin on the surface of the extruded precursor solution. The skin then collapses to generate the nanobelt fiber because of the effect of gravity and time.[24]

3.2 Removal of template from precursors membrane

To obtain pure inorganic fibers, the organic PVB template should be removed using high annealing temperatures. However, vigorous decomposition of the organics could result in the distortion of the nanobelt mats. To monitor the decomposition of PVB, FNM (precursor fiber membrane containing PVB template) was subjected to TGA under a flow of dry air. The thermogram is shown in Fig. 3a. As observed, the weight loss of the precursor fiber membrane started at 400 □, and complete decomposition of PVB was achieved at 500 □, generating a pure inorganic fiber membrane with a solid content of 50%.

Removal of the PVB template was additionally assessed by subjecting the pure PVB fiber membrane, FNM (precursor membrane) and FNM calcined at 500□. FT-IR spectroscopy analyses (Fig. 3b), and spectrum were compared. The pure PVB fiber membrane (Fig. 3b, curve 1) displays typical bands of PVB, which includes stretching vibrations of -OH at 3466 cm^{-1}, stretching vibrations of CH and CH_2 groups at 2957 cm^{-1} and C-O-C bending vibrations at 1135 cm^{-1}. FNM (precursor membrane) (Fig. 3b, curve 2) displays absorption bands characteristic of PVB/SiO_2 at 3466, 950 and 797cm^{-1} (corresponding to the stretching vibration of -OH, bending vibrations of Si-OH, and t Si-O-Si vibration, respectively). This

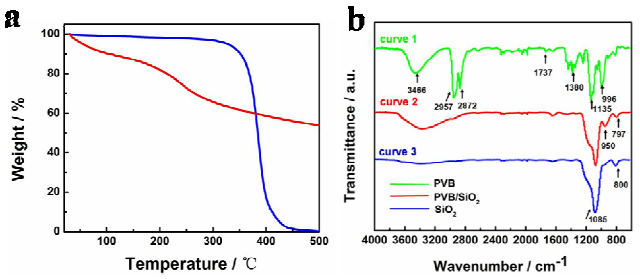

Fig. 3 (a) Thermogravimetric analysis (TGA) curve of FNM (precursor membrane). (b) Fourier transform infrared (FT-IR) spectra of the pure PVB fiber membrane (curve 1), FNM (precursor membrane: curve 2), and FNM calcined at 500□ (curve 3).

result indicates that TEOS in the precursor FNM had been hydrolyzed. In contrast, FNM calcined at 500 □ (Fig. 3b, curve 3) displays absorption bands characteristic of SiO_2 at 1085 and 800 cm^{-1}.[25,26] Thus, the FT-IR results confirms that the critical temperature for removing PVB is 500 □.

3.3 Mechanical properties of FNM

To obtain free-standing fluorescent nanofibrous inorganic membranes, the latter needs to display excellent mechanical properties. Accordingly, the mechanical properties of the prepared membrane were examined. As observed from the optical profiler results (Fig. 4a), after nitridation at 1000 □, the FNM remains smooth and flat, and features high flexibility: it could be laid flat (Fig. 4b), bent (Fig. 4c and d), or rolled (Fig. 4e) without visible damage. Furthermore, as shown in Fig. 4f, the FNM (diameter: 2 cm, thickness: 0.2 mm) could withstand a weight of 200 g without rupture. Thus, the results

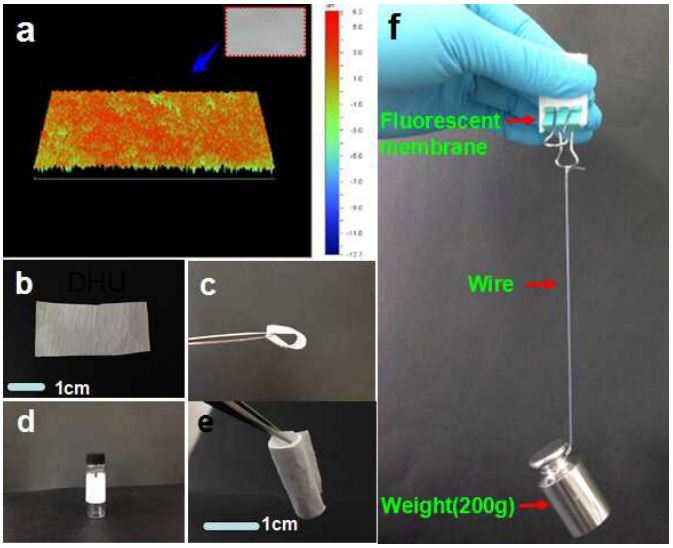

Fig. 4 (a) Optical profiler 3D interactive image of FNM nitrided at 1000℃. (b)-(e) The FNM shows great flexibility: it can be laid flat, bent, or rolled without visible damage. (f) The FNM (diameter: ~2 cm, thickness: 0.2 mm) is able to withstand weight of 200 g without rupture.

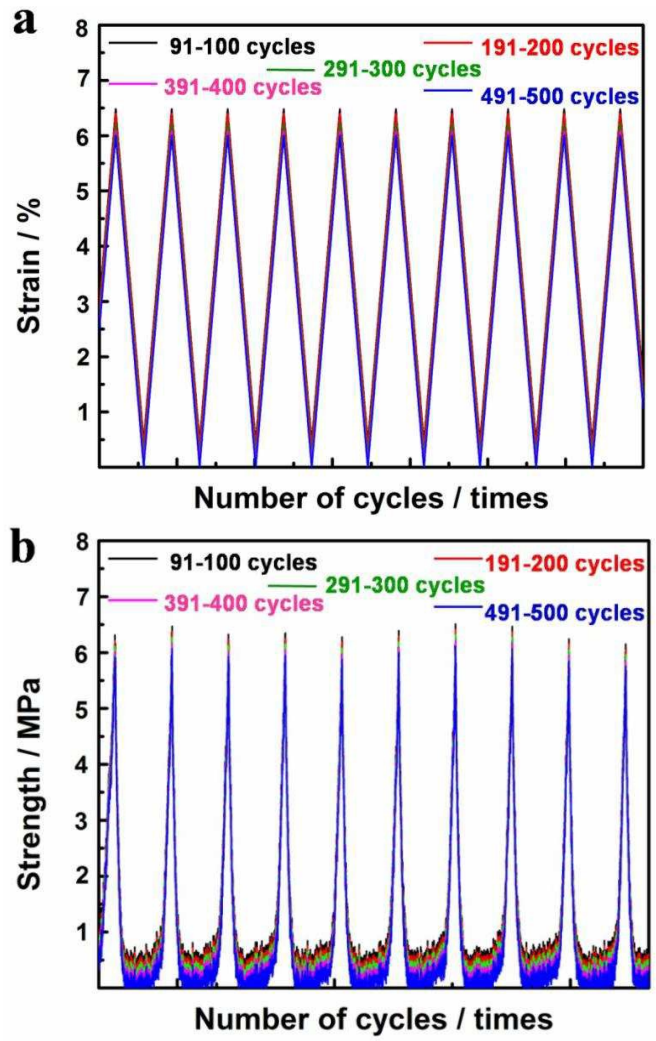

Fig. 5 Strength-strain curves of the FNM nitrided at 1000℃ recorded over 500 cycles using a universal material testing machine.

show that the FNM, prepared herein, has excellent mechanical properties.The FNM nitrided at 1000℃ was also subjected to cyclic stability tests to further evaluate its mechanical properties. Specifically, the strength-strain curves of FNM over 500 cycles were recorded using a universal material testing machine (Fig. 5a and b). Under an applied strain of 6% , the FNM retains high strength properties (6.0 MPa) even after 500 cycles.

3.4 Fluorescence properties of FNM

The emission spectrum of the FNMs prepared at varying nitridation temperatures are shown in Fig. 6a. The spectrum all exhibit a single broad band in the 400-650 nm region, with a maximum peak intensity observed at 475 nm, which can be associated with the Eu^{2+} 5d→4f transition. Furthermore, it is observed that the fluorescence intensity of FNM decreased with increasing nitridation temperatures from 1000 to 1300℃. Thus, a nitridation temperature of 1000℃ is optimal for achieving high fluorescence intensity. Furthermore, the thermal

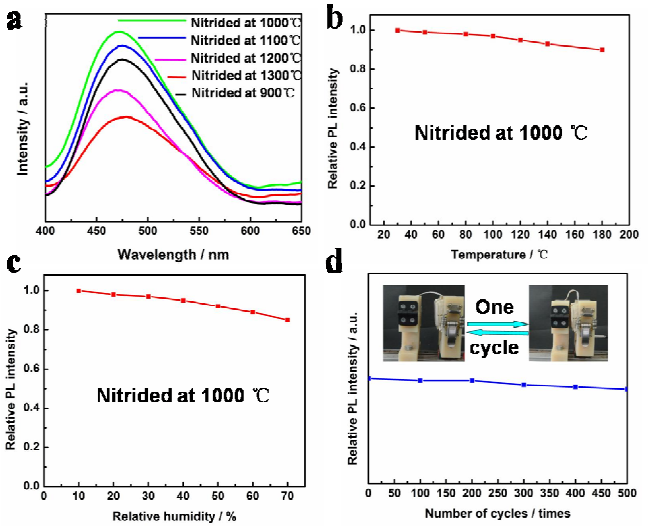

Fig. 6 (a) Variations in the photoluminescence (PL) intensity of FNMs as a function of nitridation temperatures. (b) FNM nitrided at 1000℃ as a function of heating temperature from room temperature to 180℃. (c) FNM nitrided at 1000℃ as a function of relative humidity exposure for two months. (d) FNM nitrided at 1000℃ after the cyclic bending test.

quenching of luminescence is an important parameter for phosphor materials. Fig. 6b shows the temperature dependence of the fluorescence intensity of the membranes. As observed, the PL intensity decreases slightly with increasing heating temperatures; a high PL intensity of 90% of that measured at room temperature was observed at 180℃. This result indicates that the FNM phosphor material has good thermal stability. The stability of the luminescence properties in different environments is also an important parameter for

phosphor materials. In this work, the PL intensity of the FNM was tested at different relative humidities, from 10 to 70%. As observed, 85% of the original PL intensity measured at the relative humidity of 10% is maintained after membrane exposure to varying relative humidities for 2 months (Fig. 6c). These results indicate that the FNM phosphor material has high stability in different environments. Additionally, flexible fluorescent materials are needed in many practical applications. Thus, the mechanical cyclic stability of the luminescence property is an important parameter for soft phosphor materials. Fig. 6d shows the representative result of one-cycle bending test performed on FNM nitrided at 1000 □. For the test, the FNM was first laid flat on a house built mechanical motor. Then, the FNM was bent to curvature radius of 1 cm, and subsequently flattened to its starting configuration (Electronic Supplementary Information Video S1). The PL intensity of the FNM subjected to 100, 200, 300, 400 and 500 cyclic bending was recorded. After 500 cycles, the PL intensity of the FNM is mostly unchanged, thus indicating that the fluorescence properties of the prepared FNM have excellent mechanical cyclic stability.

3.5 Function and mechanism of nitridation

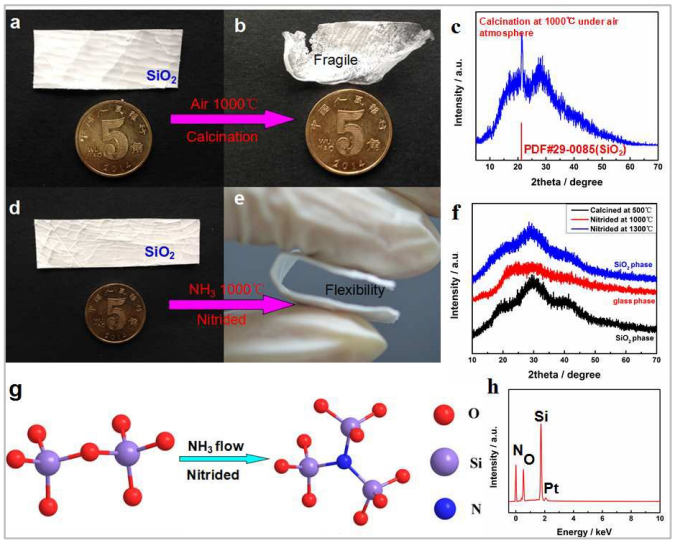

Fig. 7 (a) and (b) Photographs and (c) associated X-ray diffraction (XRD) pattern of precursor FNM calcined at 1000□ under air atmosphere. (d) and (e) Photographs of precursor FNM nitrided at 1000□ under NH_3 atmosphere. (f) XRD patterns of precursor FNM nitrided at different temperatures under NH_3 atmosphere. (g) Schematic representation of mechanism of nitridation. (h) Energy-dispersive X-ray spectroscopy pattern of FNM nitrided at 1000□ under NH_3 atmosphere.

From the above results, we can conclude that the newly prepared flexible SiO_2-based composite fluorescent nanofibrous membrane nitrided at 1000 □ has excellent mechanical properties. The superior mechanical flexibility of the nanobelt network was further confirmed through direct observation of the microstructural features of the prepared membrane and controlled trials. As determined from Fig. 2d, the excellent flexibility properties observed in the nanofibrous membrane originates from the unique ribbon-like nanostructure and well-interconnected web-like configuration, which enable the membrane network to maintain its structural integrity upon bending by releasing the applied stress at the nanoscale level.

When the precursor FNM was calcined at 1000□ under air atmosphere, it becomes fragile and shrank as shown in Fig. 7a and b. The X-ray diffraction (XRD) pattern in Fig. 7c indicates that the FNM featured distinct crystalline features following calcination at 1000□ under air atmosphere. In contrast, as shown in Fig. 7d and e, when the precursor FNM was nitrided at 1000□ under NH_3 atmosphere, the resulting membrane exhibits excellent flexibility, which instead of obvious crystallzation of glass phase.

A mechanism is proposed for the beneficial influence of nitridation on the mechanical properties of FNM as illustrated in Fig. 7g. NH_3 prevents the precursor FNM from crystallizing and some of the oxygen atoms are replaced by the nitrogen atoms present in the precursor FNM. Specifically, the FNM displays crystalline glass features upon heating at 1000□ under NH_3 atmosphere for 5h, which is consistent with the XRD pattern shown in Fig. 7f. The energy-dispersive X-ray spectroscopy results in Fig. 7h indicated that some of the oxygen atoms are replaced by nitrogen atoms. The above result also can be proved by XPS of FNM. Fig. S3 indicates that the presence of N1s with binding energy of 398 eV, which is attributed to the Si-N bond. All of the above results indicate that nitridation is contributed to improve the mechanical properties of FNM. The results are consistent with investigations performed on oxynitride glass.[19-23] These studies reveal that the replacement of oxygen with nitrogen improves physical properties such as fracture toughness, microhardness, refractoriness, and chemical durability.

3.6 The application of FNM for the remote packaging

In recent years, the remote package developed rapidly, especially the conventional florescence layer made up of phosphor and epoxy used in remote packaging white LEDs, which can greatly improve the luminous efficiency and lifespan. But there are two problems to be solved: one is that the uneven dispersion of phosphor powders in the resin, decreases the luminous efficiency at a certain extent (Fig. S4a); Another problem is brought by easy aging of the resin, which will significantly shorten the lifespan of the LEDs. It is useful to develop a novel nanobelt phosphor membrane, which can be used in remote packaging and solve the problems that brought by phosphor powders. First, a uniform fiber distribution ensures the excitation light transmittance which can greatly improve the luminous efficiency. Secondly, the free-standing nanobelt phosphor membranes are composited with pure inorganic phase, which can greatly prolong the lifespan of white LEDs (Fig. S4b). In our experiment, as shown in Fig. 8. Firstly, we purchased a purple light chip (Fig. 8(a)), it was surrounded by a high temperature resistant ceramic gasket. Secondly, we cut the phosphor membrane to the size of 1cm × 1 cm, to realize the remote packaging combined with

the purple light chip (Fig. 8(b)). At last, under the 100 mA driving current, the white light was obtained.

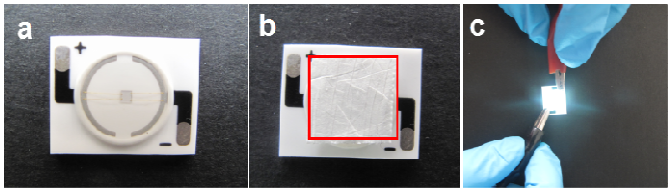

Fig. 8 (a) the purple light chip; (b) the FNM combined the purple light chip to realize the remote packaging of white LED; (C) the white LED under 100 mA drive current.

4. Conclusions

Novel flexible SiO_2-based fluorescent nanobelt membranes were successfully prepared by a simple and versatile electrospinning process combined with gas reduction nitridation. The resulting FNM has high flexibility, and retains a high strength of 6.0 MPa even after 500 cycles. The excellent results strongly indicate the great potential of the fluorescent inorganic membranes, prepared herein, as fluorescent materials in flexible display technologies and the remote packaging of white LED.

Acknowledgements

We gratefully acknowledge financial support from the NSF of China (No. 51172042), MOE of China (IRT 1221, Grant Nos. 111-2-04, and 2232014A3-06), STC of Shanghai (Grant Nos. 13JC1400200, and 15ZR1401200), SRFDP (20110075130001), Innovation Fund of MSLA (EG2015049) and Eastern Scholar.

References

1 E. Downing and R. M. Macfarlane, *Science*, 1996, **273**, 1185.
2 S. Helmut, P. Pavel, K. Karsten, H. Markus, *Chem. Mater.*, 2007, **19**, 1396.
3 Y. X. Gu, Q. H. Zhang, Y. G. Li and H. Z. Wang, *J. Mater. Chem.,* 2011, **21**, 17790.
4 S. Coe, W. K. Woo, M. Bawendi, V. Bulovic, *Nature*, 2002, **420**, 800.
5 C. Feldmann, T. Justel, C. R. Ronda, P. J. Schmidt, *Adv. Funct. Mater.,* 2003, **13**, 511.
6 X. F. Duan, Y. Huang, Y. Cui, J. F. Wang, C. M. Lieber, *Nature*, 2001, **409**, 66.
7 J. P. Hu, X. F. WangY, B. Ding, J. Y. Lin, J. Y. Yu, G. Sun, *Macromal. Rapid Comm.,* 2011, **32**, 1729.
8 X. M. Hu, Q. Chen, D. Zhou, J. Cao, Y. J. He, B. H. Han, *Polym. Chem.,* 2011, **2**, 1124.
9 J. Chen, L. N. Xu, W. Y. Li, X. L. Gou, *Adv. Mater.* 2005, **17**, 582.
10 X. F. Wang, B. Ding, G. Sun, M. R. Wang, J. Y. Yu, *Prog. Mater. Sci.,* 2013, **58**, 1173.
11 Y. Q. Liu, X. P. Zhang, Y. N. Xia and H. Yang, *Adv. Mater.,* 2010, **22**, 2454.
12 H. Wu, Y. Sun, D. D. Lin, R. Zhang, C. Zhang, W. Pan, *Adv. Mater.,* 2009, **21**, 227.
13 S. Agarwal, A. Greiner and J. F. Wendorff, *Adv. Funct. Mater.,* 2009, **19**, 2863.
14 H. W. Song, H. Q. Yu, G. H. Pan, X. Bai, B. Dong, X. T. Zang, S. K. Hark, *Chem. Mater.,* 2008, **20**, 4762.
15 Z. Y. Hou, C. X. Li, J. Yang, H. Z. Lian, P. P. Yang, R. T. Chai, Z. Y. Cheng, J. Lin, *J. Mater. Chem*., 2009, **19**, 2737.
16 G. P. Dong, X. D. Xiao, X. F. Liu, B. Qian, Q. Zhang, G. Lin, Z. J. Ma, D. P. Chen, J. R. Qiu, *J. Electrochem. Soc.,* 2009, **156**, J347.
17 G. G. Li, Z. Y. Hou, C. Peng, W. W. Wang, Z. Y. Cheng, C. X. Li, H. Z. Lian, J. Lin, *Adv. Funct. Mater.,* 2010, **20**, 3446.
18 S. Y. Huang, H. Wu, M. Zhou, C. S. Zhao, Z. F. Yu, Z. C. Ruan, W. Pan, *NPG Asia Mater.,* 2014, **6**, e86.
19 Z. W. Luo, A. X. Lu, G. Qu, Y. J. Lei, *J. Non-cryst. Solids*, 2013, **362**, 207.
20 C. J. Brinker, D. M. Haaland, *J. Am. Ceram. Soc*., 1983, **66**, 758.
21 M. R. Reidmeyer, M. Rajaram, D. E. Day, *J. Am. Ceram. Soc*., 1986, **85**, 186.
22 P. H. Mutin, *J. Sol-gel Sci. Techn*. 1999, **14**, 27.
23 B. Wang, B. S. Kwak, B. C. Sales, J. B. Bates, *J. Non-cryst. Solids,* 1995, **183,** 297.
24 D. H. Reneker, A. L. Yarin, *Polymer,* 2008, **49**, 2387.
25 M. Guo, B. Ding, X. H. Li, *J. Phys. Chem. C.*, 2010, **114**, 916.
26 B. Ding, E. Kimura, T. Sato, *Polymer*, 2004, **45**, 1895.

Graphical abstract

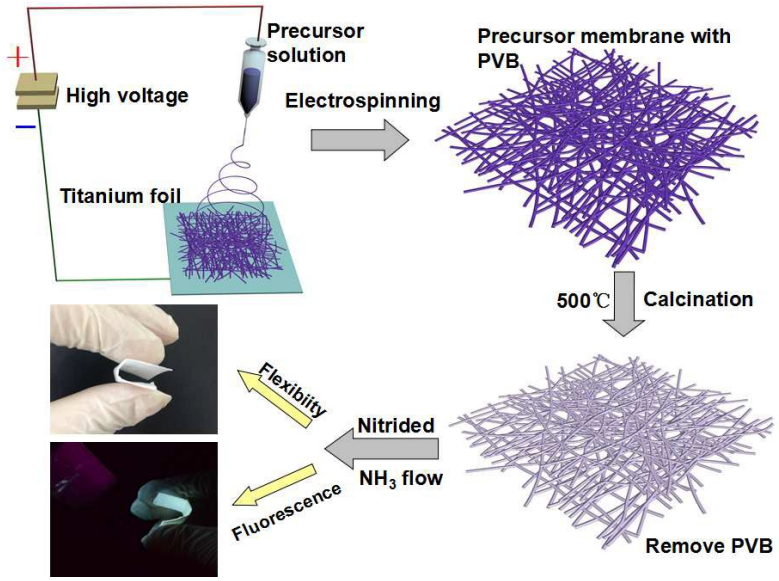

Novel flexible SiO_2-based fluorescent nanobelt membranes were successfully prepared by a simple and versatile electrospinning process combined with gas reduction nitridation. The resulting FNM has high flexibility, and retains a high strength of 6.0 MPa even after 500 cycles. The excellent results strongly indicate the great potential of the fluorescent inorganic membranes, prepared herein, as fluorescent materials in flexible display technologies and the remote packaging of white LED.